The VST telescope primary mirror safety system: simulation model and mechanical implementation

Francesco Perrotta, Francesco Martelli, Matteo Ottolini, Giancarlo Parodi, Pietro Schipani, et al.

Francesco Perrotta, Francesco Martelli, Matteo Ottolini, Giancarlo Parodi, Pietro Schipani, Sergio D'Orsi, Davide Fierro, Carmelo Arcidiacono, "The VST telescope primary mirror safety system: simulation model and mechanical implementation," Proc. SPIE 7738, Modeling, Systems Engineering, and Project Management for Astronomy IV, 773820 (5 August 2010); doi: 10.1117/12.856597

SPIE.

Event: SPIE Astronomical Telescopes + Instrumentation, 2010, San Diego, California, United States

The VST telescope primary mirror safety system: simulation model and mechanical implementation

Francesco Perrotta*[a], Francesco Martelli[b], Matteo Ottolini[b], Giancarlo Parodi[b], Pietro Schipani[a], Sergio D'Orsi[a], Davide Fierro[a], Carmelo Arcidiacono[c]
[a]INAF-Osservatorio Astronomico di Capodimonte, Salita Moiariello 16, I-80131, Napoli, Italy
[b]BCV progetti s.r.l., Via Sant'Orsola 1, 20123, Milano, Italy
[c]INAF – Osservatorio Astrofisico di Arcetri, Largo Enrico Fermi 5, I-50125 Firenze, Italy

ABSTRACT

The VST telescope is a wide field survey telescope being installed at Cerro Paranal (Chile). Due to the geological nature of the area, telescopes in Chile are always submitted to unpredictable and sometimes severe earthquake conditions. In order to clarify some aspects of VST telescope seismic behavior not well represented by linear procedures like Response Spectrum Analysis, a transient nonlinear analysis of the whole telescope has been foreseen. A mixed approach Finite Element - Matlab-Simulink has been introduced and a linear FE model of the telescope has been developed, with all nonlinear devices sources modelled as linear elements. The FE model has been exported to Simulink, using a space state representation. In Simulink all nonlinearities are appropriately modeled and a base excitement corresponding to accelerograms compliant with Paranal MLE response spectrum is applied. Resulting force-time histories are then applied to a detailed finite element model of mirror, to compute stress field. The paper describes both Simulink and mirror FE analysis, giving also an overview of the actual safety system mechanical implementation, based on analysis results.

Keywords: Telescope, Simulink, Seismic Analysis, Finite Elements

1. INTRODUCTION

The VST is a 2.6-m F/5.5 modified Ritchey-Chrétien telescope to be installed at Cerro Paranal, Northern Chile. This area is known for high magnitude, medium frequency earthquakes[1]. Therefore a considerable design effort has to be made in order to achieve an optimal primary mirror anti-earthquake protection.

The common way to investigate earthquake-related stress and deformation fields on a telescope structure is to perform a Response Spectrum Analysis (RSA). This has also been done initially for the VST telescope. However, after careful examination of RSA results and the implementation of a simplified nonlinear transient model[2], it has been decided to perform a nonlinear transient analysis of the whole telescope with the aim to clarify some aspects of VST telescope peculiar dynamics not well represented by linear procedures.

Two approaches were possible for this analysis:

- Traditional approach: develop a full nonlinear finite element (FE) model of the telescope and run a transient analysis inside ANSYS/NASTRAN, possibly reducing the number of degrees of freedom using sub structuring/sub modeling techniques (Guyan reduction, component mode synthesis, superelement analysis)
- Mixed approach: develop a linear FE model of the telescope with all the nonlinear devices represented by linear elements whose stiffness is the initial stiffness of the nonlinear force-displacement curve and then transport this model inside Matlab/Simulink, with a space state representation of the FE model. All nonlinearities are then appropriately built and a transient analysis is run inside Simulink.

*perrotta@na.astro.it

Modeling, Systems Engineering, and Project Management for Astronomy IV,
edited by George Z. Angeli, Philippe Dierickx, Proc. of SPIE Vol. 7738, 773820
 · doi: 10.1117/12.856597

The second approach has been preferred, due to high number of elements and node of the FE model and the consequent computing power and time consuming activities that should be performed during both pre- and postprocessing of a full nonlinear transient analysis on a FE model. Moreover, a dedicated software, developed by ESO, could be adapted in order to export the FE model to the Simulink model, speeding up the procedure completion.

2. PRIMARY MIRROR CELL DESCRIPTION

The M1 support system consists of an axial and a lateral part[3]. The axial support system acts along the optical axis (cell Z axis) and is based on 84 supports. 81 of them (axial actuators) are electro-mechanical push-only devices: a motorized screw moves axially a piston on which there are six helical springs in parallel. The remaining 3 (axial fixed points) have the same mechanical structure, but they are fixed during telescope operation and provided with stiffer spring: their function is to define the axial position of the mirror, with respect to the cell. The presence of a mechanical load cell protection device against excessive loads makes the force-displacement characteristic of the supports nonlinear.

The lateral support system acts along cell Y axis, orthogonal to telescope altitude axis (cell X axis). It is based on 24 astatic lever supports surrounding the mirror (astatic levers). The stiffness of such a system is virtually zero; therefore any earthquake induced oscillations of the mirror inside the cell are in principle not restrained by the astatic levers: they act like a series of masses attached to the mirror. Three tangential fixed points define the position of the mirror in the XY plane (lateral fixed points): they are based on a stiff spring and have a limited load capacity, up to 800 N each. Further increase of mirror lateral displacement doesn't change the load on fixed points.

Fig.1 shows the mirror in the cell, surrounded by support system and safety devices

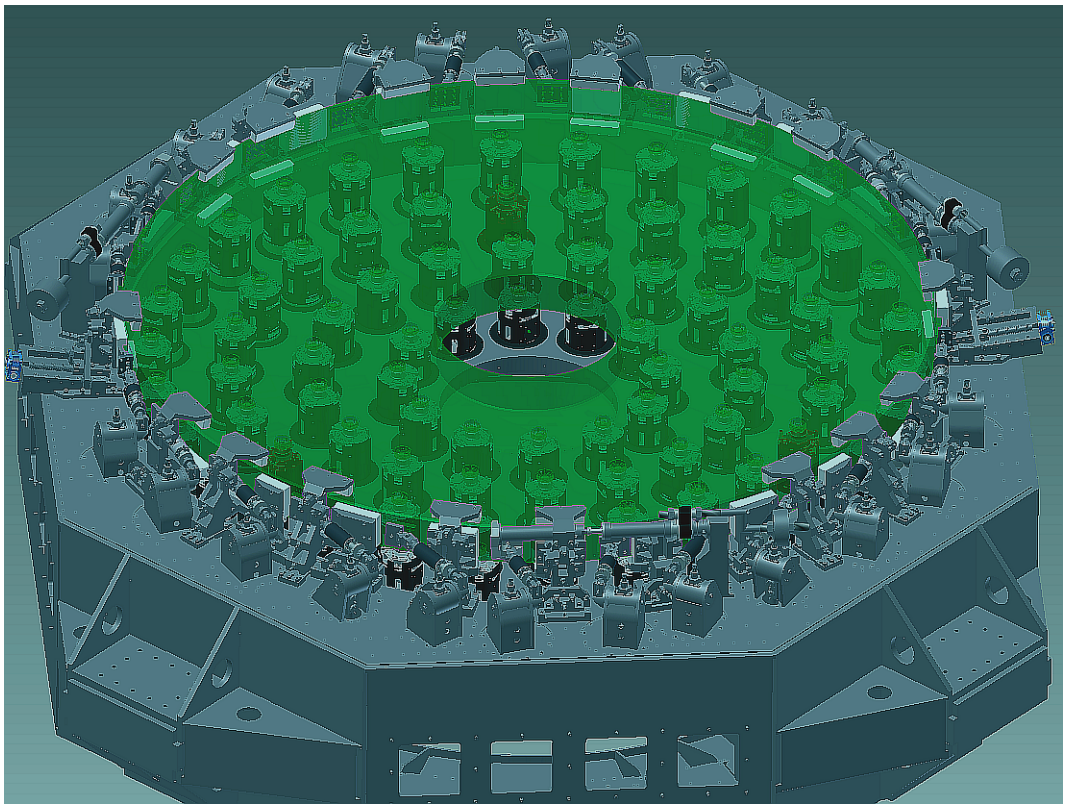

Fig. 1 VST primary mirror cell

The axial and lateral safety systems are constituted by a set of steel supports with an interface toward the mirror made by appropriate elastomeric materials, at a distance form the mirror of about 0.5-1 mm. Lateral (radial) safety devices are radially disposed around the mirror, acting ideally along the direction of a mirror radius. Axial safety devices act along optical axis (cell Z axis) both on mirror top and bottom side: in some location however they are not present on both sides due to mechanical constraints.

Initial safety system design variables were support number and support stiffness (elastomeric material type, support dimensions). As a constraint, the mirror cannot translate more than 4 mm with respect to the cell in all directions, otherwise mechanical interferences with cell devices could arise. Moreover, the stress field inside the mirror cannot exceed 4 MPa, including operational stress due to gravity and thermal gradients thus limiting the amount of "braking" force that can be exerted by safety devices on the mirror.

As first design step, a number of safety devices with a predefined contact surface on the mirror has been located inside the cell, actually the maximum possible number taken into account all the possible interferences with other devices. This number could be reduced modifying the stiffness of the elastomers used, without violating the constraint previously mentioned.

Fig. 2 shows initial radial and axial safety devices distribution and numbering.

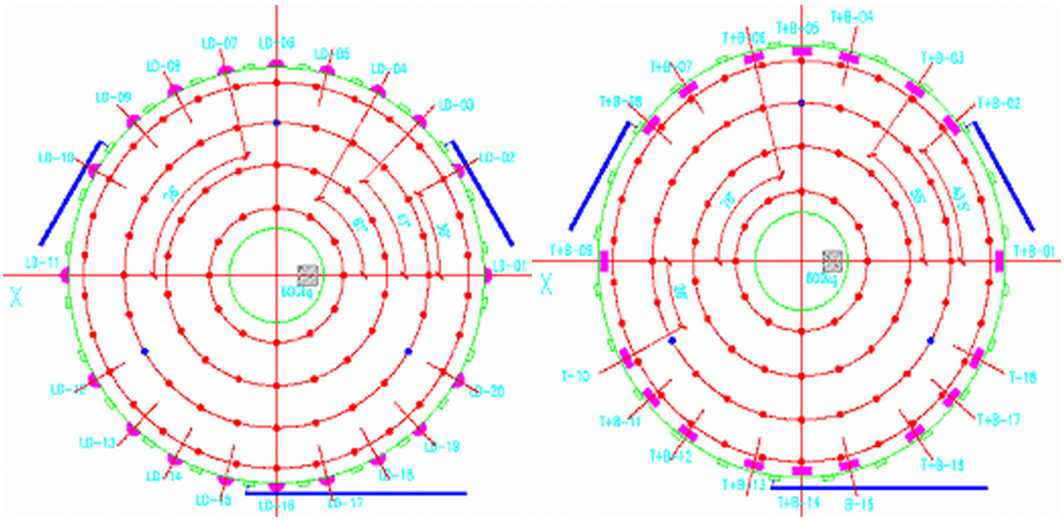

Fig. 2 Radial (*left*) and axial (*right*) safety devices disposition and numbering: T=Top, B=Bottom - mirror seen from above

Fig. 3 shows a detail of the radial and axial safety supports: radial safety devices have different sizes to prevent any interference with other devices not shown in the figure.

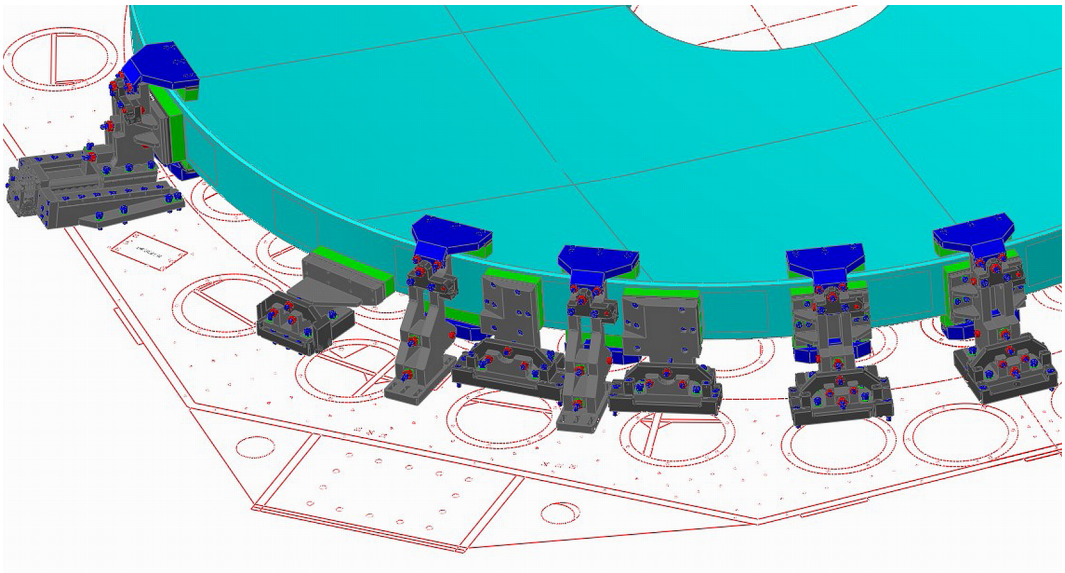

Fig. 3 Detailed view of safety devices assemblies

The 17 top pads, the 16 bottom pads and the 20 radial pads are foreseen to operate on the mirror surface through an assembly of two types of elastomers, polyurethane U42 and polyurethane U315: the former has the function to absorb mirror kinetic energy allowing for a gradual deceleration of the mirror, therefore limiting breaking forces values; the latter (thickness: 3 mm), is harder than U42 and its function is to avoid scratching of the U42 caused by the contact with lateral mirror surface.

3. DYNAMIC MODEL

VST telescope can be seen as a lightly damped structure, where the damping comes from losses at the joints and material losses. In this case it's possible to restructure the system of equations representing the finite element model in terms of individual modes of vibration, using a particular type of damping called "proportional damping"[4].The solution starts with deriving the un-damped equations of motion in physical coordinates. The next step is solving the eigenvalue problem, yielding eigenvalues (natural frequencies) and eigenvectors (mode shapes). The model is then transformed to the modal coordinate system, by operating on the original equations with the eigenvector matrix: the original un-damped coupled equations of motion are transformed to the same number of un-damped uncoupled equations. Each uncoupled equation represents the motion of a particular vibration mode of the system. It is at this step that proportional damping is applied.

To reduce the computing time model reduction techniques are applied in two steps. The first is reducing the number of degrees of freedom of the model from the original set to a new set which includes only those degrees of freedom where forces are applied and/or where responses are desired. The second step is reducing the number of modes of vibration used for the solution by considering the cumulative effective modal masses and the maximum earthquake significant frequency.

The result of the procedure described is a mechanical system in the well known Space State form:

$$\dot{x} = Ax + Bu$$
$$y = Cx + Du$$

where x is the vector of the state space variables, u is the vector of the mechanical system external forces/disturbances, y the vector of the desired output.

The matrices A (system matrix), B (control matrix) and C (observation matrix) are derived as outlined by Schipani Perrotta and Marty[5]. The modal damping ratio ζ is 0.01, as for Paranal telescope response spectrum[1].

Fig 4 shows the deformed shape of the telescope and pillar for 2nd and 3rd vibration mode.

4. SPACE STATE TRANSFORMATION

Once the number of eigenvectors has been chosen, in order to define completely the space state model it is necessary to determine which are the desired input/output nodes (and in general also the derived quantities, such as speeds and differential displacements of the nodes).

All the nodes representing the devices physically attached to the mirror or potentially in contact with it, and the node representing ground point, connected rigidly to pillar base (Fig. 3 (*right*)), are input nodes. The rotational degrees of freedom of the "ground" node are blocked, keeping free the translational ones: the earthquake accelerations are applied to these DoFs, transmitted to pillar base and then to the telescope.

The State Space Model of the telescope structure is based on the first 200 modes: 197 flexible modes and 3 rigid body modes, translation along global z, x, y direction (global coordinate system coincides with cell coordinate system when telescope points toward zenith). These are the modes corresponding cumulatively to more than 90% of modal masses along z, x, y direction, giving a response up to 150 Hz. According to Paranal MLE response spectrum, the highest earthquake significant frequency is about 40Hz[3].

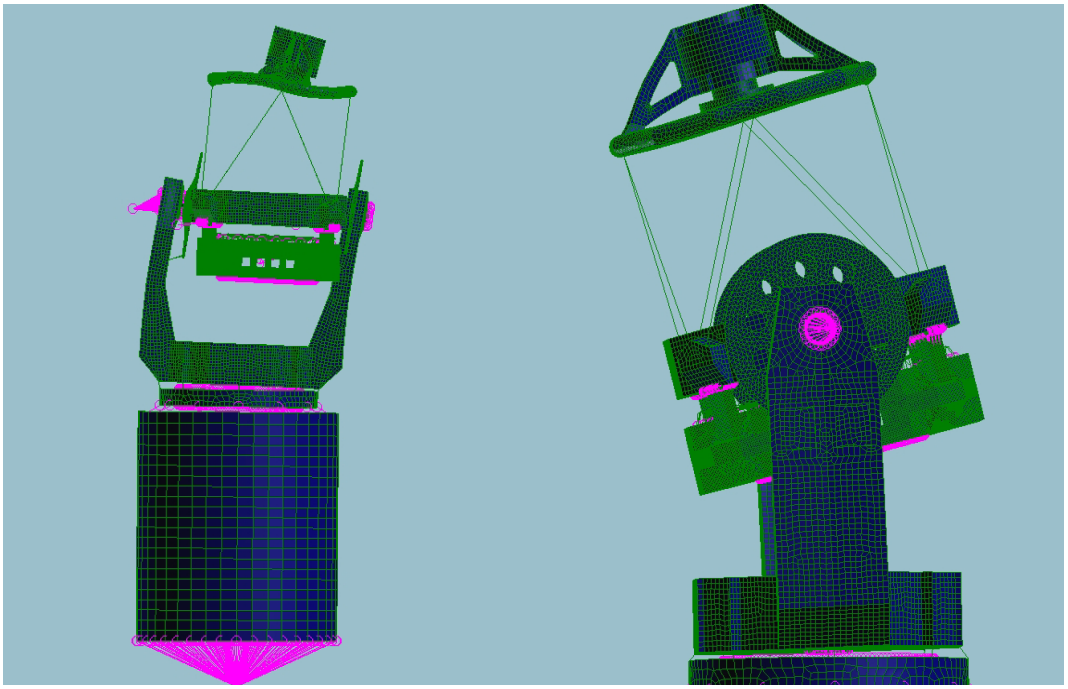

Fig. 4 Telescope and pillar deformed shape for 2nd (*left*) and 3rd (*right*) vibration mode

4.1 Local coordinate system specification

Each device that can be in contact with the mirror during an earthquake is modeled in NASTRAN/ANSYS as a uni-axial linear element: that is, no stiffness in direction normal to element axis, and no rotational stiffness. For each element a local coordinate system is defined, with the origin in the element node "1", the node on the element toward the cell, axis "U" from node 1 to node 2, with node 2 attached to the mirror. The element length variation, ΔL, can be calculated as the difference between displacement of node 2, U2, and displacement of node 1, U1:

- ΔL >0 means U2-U1>0: the element is subject to a tensile load.

- ΔL <0 means U2-U1<0: the element is subject to a compressive load.

4.2 Space state model inputs

The input vector u includes (i) 154 forces for the devices attached or in contact with the mirror; positive forces are applied along positive direction of 1-2 axis on node 2, along negative direction on node 1 (these forces are transformed into global telescope coordinate system using matrices B and D), (ii) input force for the base-excitation node of the model, along x, y, z global coordinate system directions.

4.3 Space state model outputs

The output vector y includes (i) 154 differential displacements (element length variations) for the devices connected or in contact with the mirror, (ii) M1 rigid body motions (3 translations and 3 rotations), (iii) ground input accelerations.

5. SIMULINK MODEL

The element length variations, ΔL, output from the VST space state model, are sent to the appropriate sub-blocks, that compute the forces to be applied to the mirror according to the nonlinear characteristic curve of each device (Fig. 5).

Fig. 6 (*left*) shows the scheme of the Axial Fixed Points block. The schemes of the blocks representing the other devices are based on a similar structure, although with higher complexity. The axial fixed points are introduced in the FE model as linear springs attached to the mirror, whose stiffness equals to the initial compressive stiffness of the corresponding physical device acting on the mirror, as computed from the force-displacement diagram in Fig. 6 (*right*): the axial fixed points do not exert any traction force on the mirror.

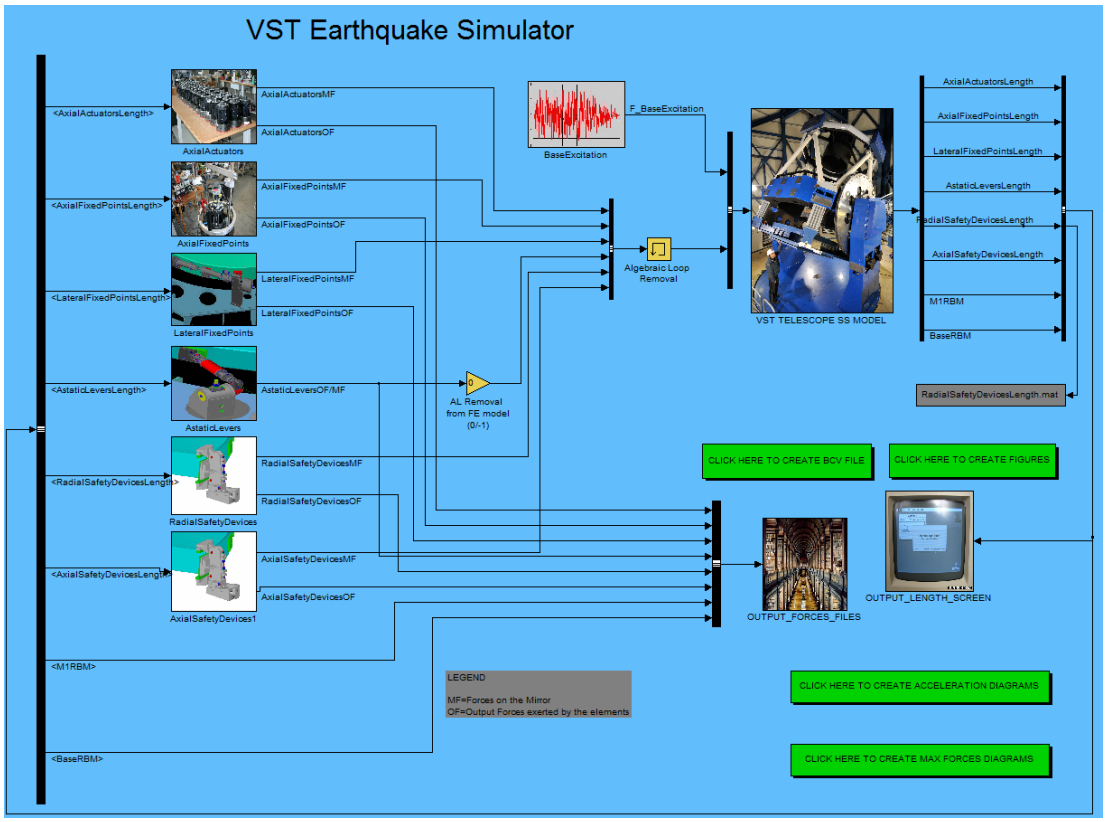

Fig. 5 VST Simulink earthquake model

The former is used to compute a force to be applied to the mirror (and correspondingly, to the cell) that shall be equal and opposite to the force exerted by the linear spring of the axial fixed point device in the FE model, eliminating the contribution of this spring to mirror dynamics. The latter is used to apply to the mirror a force deriving from the interaction between the mirror and the corresponding fixed point, following the theoretical force-displacements curve. The two functions can be of course combined into a single one but, for output purpose and for convenience in the debugging phase, they have been kept separate.

Block input is the differential displacement ΔL of the nodes representing the axial actuators, block outputs are the force to be applied to the mirror (including the linear force needed to null the force exerted by the FEM spring) and the nonlinear force to be recorded in the output file.

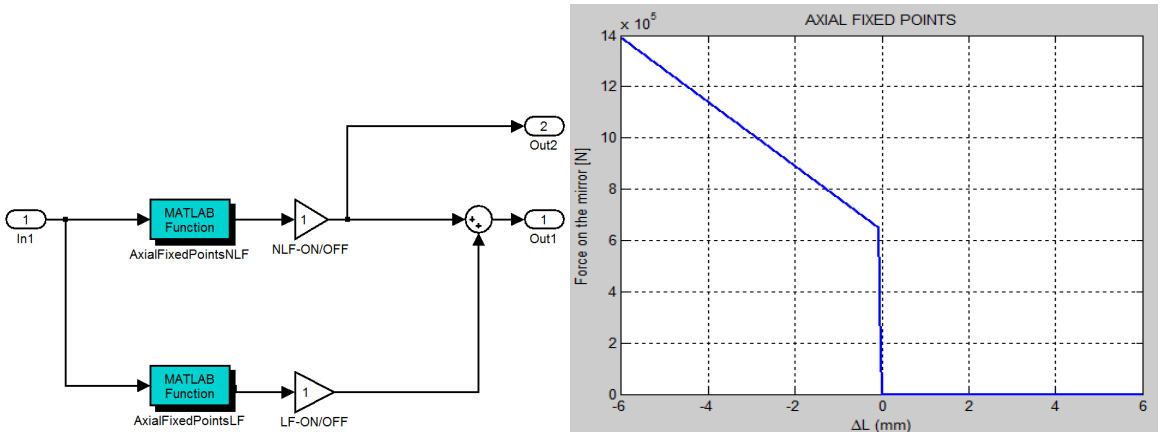

Fig. 6 Axial Fixed Points block insight (*left*) and nonlinear force-displacement curve (*right*)

6. ACCELERATION TIME-HISTORIES

A total of ten simulated accelerograms have been generated (Fig. 7), five from the Paranal horizontal response spectrum[6] and five from the Paranal vertical response spectrum: the latter has been computed from the former following the provisions of the Eurocode 8[7].

The acceleration time-histories were computed using the SIMQKE_GR. (rel. 1.4), graphical interface for the program SIMQKE-1 (SIMulation of earthQuaKE ground motions), developed at Civil Engineering Department of University of Bologna (Italy).

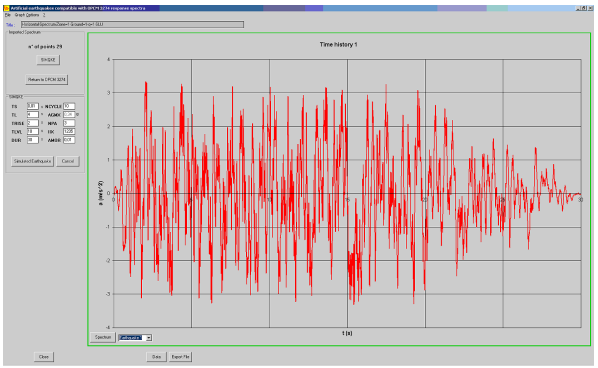

Fig. 7 Acceleration (m/sec^2) vs. time (sec) – vertical time history 3.

7. TRANSIENT SIMULATION

Three set of three acceleration-time history, one from the vertical set, and two different from the horizontal set have been chosen and applied as input in the Simulink model. Each analysis has been repeated for two configurations, considered as the most significant: mirror pointing toward horizon and mirror pointing toward zenith. Analysis results include the force-time history for all the elements in contact with the mirror, along with mirror acceleration and relative displacement with respect to the cell. Figs. 8-10 show mirror accelerations along x,y,z global axes for both configurations.

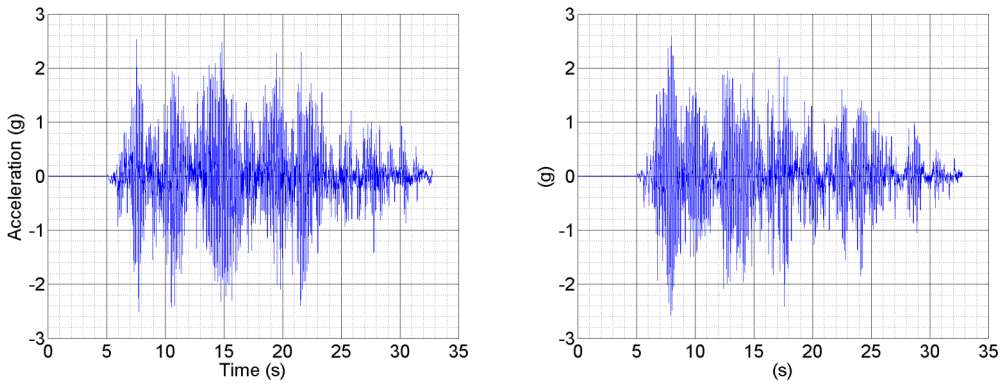

Fig. 8 Mirror acceleration along x axis: telescope pointing to horizon (*left*) and zenith (*right*)

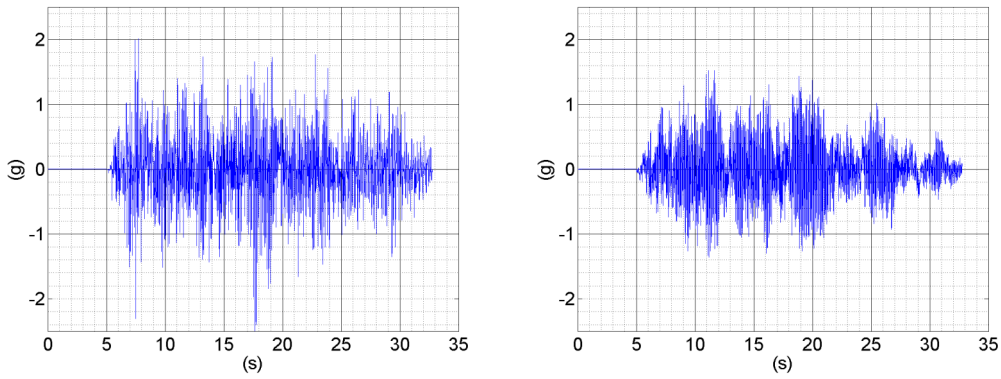

Fig. 9 Mirror acceleration along y axis: telescope pointing to horizon (*left*) and zenith (*right*)

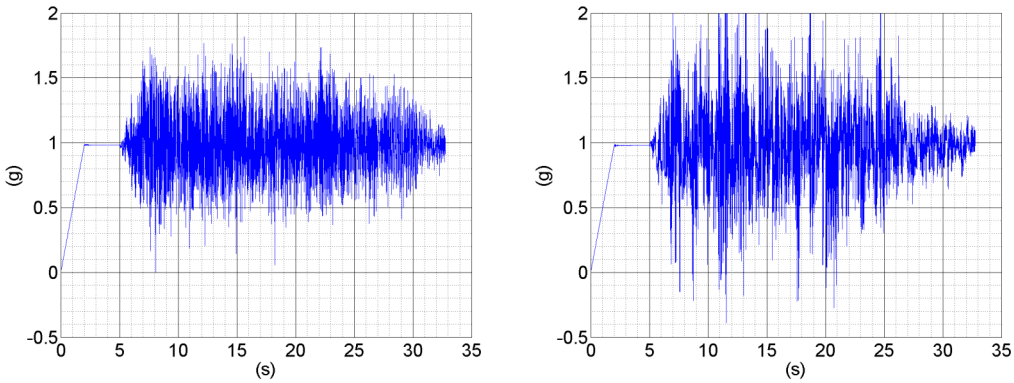

Fig. 10 Mirror acceleration along z axis: telescope pointing to horizon (*left*) and zenith (*right*)

The linear varying part of mirror acceleration in Fig. 10 is needed in order to avoid spurious accelerations on the model due to a sudden application of the gravity and earthquake load on it: gravitational load grows steadily until gravity normal acceleration is reached, keeping the structure under "quasi-static" conditions. Then ground acceleration as computed with the SIMQKE_GR. is summed to gravity. This has been considered the optimal way to apply both gravity and time-dependent load on telescope structure, avoiding unrealistic "overshooting" of model response, with respect to the physical system[8].

8. MIRROR FINITE ELEMENT ANALYSIS

The histories of forces and accelerations have been applied as external forces (and acceleration field) to a model of the mirror, with a series of static analysis. (Fig. 11).

A solid global model of the mirror has been realized. Proper surfaces corresponding to the nominal interfaces with supporting assemblies have been defined onto the mirror model: circular glass regions under INVAR pads for axial actuators and axial fixed points, "rectangular" free surfaces of modeled glued INVAR pads for astatic levers and lateral fixed points, glass target surfaces for contact pairs resulting from the activation of axial and radial safety devices.

In principle a separate static analysis should be performed for each time step resulting from transient analyses. Practically, in reason of the overwhelming computational effort resulting from a similar approach, only a significant subset of time steps has been selected to be processed. It should be noticed that this approach neglects any additional damping effect related to the motion of the system, not already taken into account in the Simulink model. Forces exerted at the same instant at all interfaces have been applied simultaneously on relative application surfaces as nominal distributed pressures. Displacement constraints necessary to prevent rigid-body motions have been specified and a program-calculated acceleration field capable of counterbalancing applied loads and grant zero reactions at constraint

points (inertia relief) has been imposed, in order to reproduce the same conditions of "space free body motion" observed in transient analyses. Furthermore the program-calculated acceleration field (in terms of translational and rotational accelerations) has been compared with acceleration field provided by Simulink model results at each step, validating solid modeling and application points/directions of nominal forces. Program-calculated values matched with good precision reference ones. A proper number of static analyses have been performed for each of the six time history sets available.

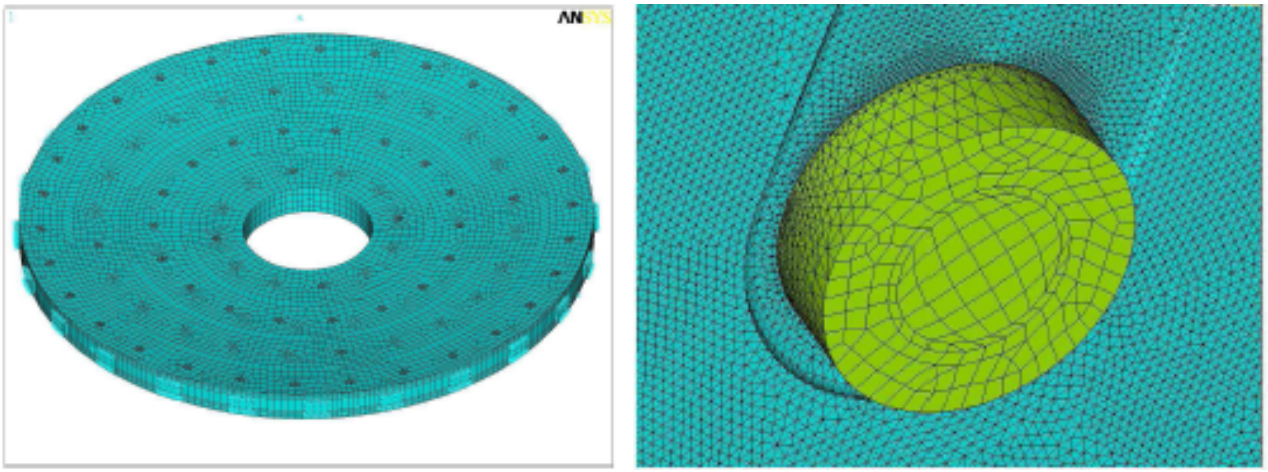

Fig. 11 Mirror global model (*left*) and axial actuators pad area sub model (*right*)

In order to process the vast amount of collected results an ad-hoc automatic post-processing procedure has been set up. Principal stresses of all analyzed load steps for each time history have been enveloped and a set of different locations where maximum (and minimum) values occur have been identified; the corresponding set number retrieved. The above mentioned sensible locations, detected on the global M1 FEM, can be divided in "global stress regions" and "local stress regions", according to the following criteria: global stress regions are located in zones reasonably far from global model singularities so that they fit the stress pattern (and stress values) on large fields in a sufficiently correct way. Local stress regions are located near model singularities (ex. abrupt material transitions, zones where loads are applied, geometrical stress raisers) and do not immediately represent the exact stress pattern, they should be treated as poorly meaningful in numerical value, conversely they are essential to highlight critical regions where a local sub-model is required to deep investigate stress pattern. Local stress regions are indeed located mainly near modeled INVAR lateral pads.

Since global model element size is not adapted to catch neither machined surfaces in glass nor pad adhesive interfaces, local refined sub-models with small sized elements have been implemented, including chamfers, machined details and fillet radiuses. Local sub-models boundary conditions in terms of displacements are obtained directly from global models. Whenever also results derived from local models give rise to unreasonable stress peaks resulting from topological singularities and abrupt material transitions, especially where adhesive layers cannot be modelled (because of incompatibilities with general element size) numerical stress values have been scaled by proper reduction factors, evaluated through separate models.

Fig. 12-13 show stress patterns around safety devices for the configuration mirror pointing toward horizon.

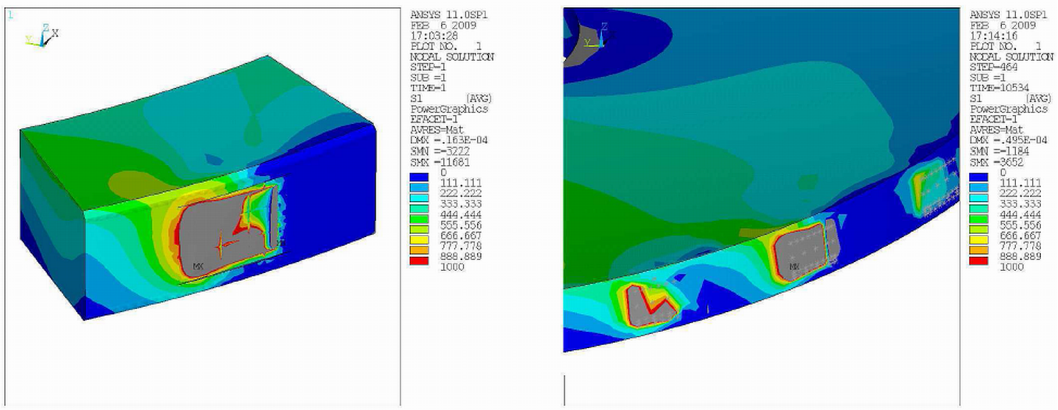

Fig. 12 Seismic tensile stress distribution around an astatic lever interface: local model (*left*) and reference global model (*right*). - mirror pointing toward horizon

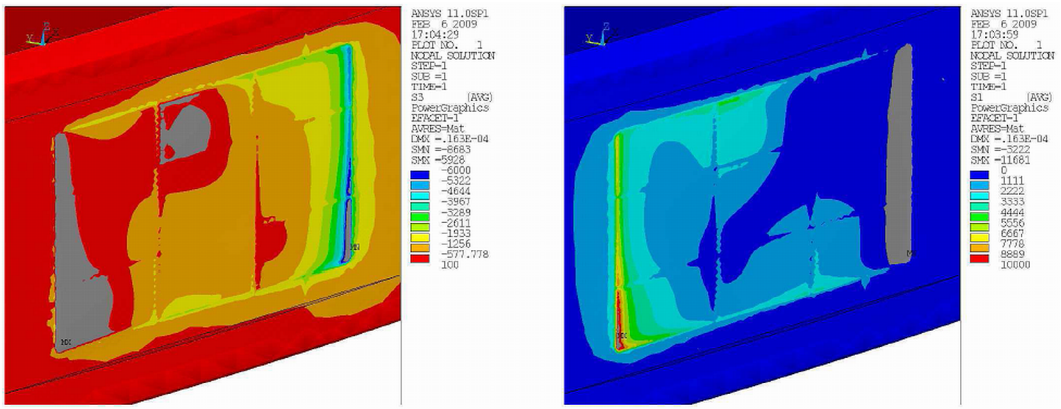

Fig. 13 Seismic compressive stress distribution around an astatic lever interface: local model (*left*) and reference global model (*right*). - mirror pointing toward horizon

9. CONCLUSIONS

The earthquake simulation procedure for the VST telescope has been presented. Due to the complexity of the support and safety systems, a traditional approach based on response spectrum analysis was unsatisfactory to evaluate the forces on the mirror during a seismic event. A transient nonlinear analysis has been carried out, exporting the FE linear model to Simulink, with a space state representation. In Simulink all nonlinear devices have been properly modelled and a simulation in the time domain has been performed. The procedure allowed the computation of the time histories for the forces applied to the mirror by all the support and safety devices.

Then, the forces computed have been used as input for a static analysis of the mirror: force-time histories have been applied to a detailed 3D mirror model. The results of the analysis have shown that the mirror stress field is inside safety margins.

10. ACKNOWLEDGEMENTS

The authors would like to thank Michael Mueller and Franz Koch from the European Southern Observatory, who suggested to model telescope nonlinear elements inside Simulink and provided the software for the export of the telescope linear FE model to Simulink.

REFERENCES

[1] Koch, F., "Analysis Concepts for Large Telescope Structures under Earthquake Loads", Proc. SPIE 2871, 117-126 (1997).

[2] Perrotta, F., "Earthquake safety system design for a telescope primary mirror", Proc. SPIE 7017, 70171S (2008).

[3] Schipani, P., D'Orsi, S., Ferragina, L., Fierro, D., Marty, L., Molfese, C., Perrotta, F., "Active optics primary mirror support system for the 2:6m VST telescope", Applied Optics Vol. 49, No. 8 (2010).

[4] Hatch, M., [Vibration Simulation using Matlab and Ansys], Chapman & Hall/CRC, Boca Raton London New York Washington D.C., 1-4 (2001).

[5] Schipani, P., Perrotta, F., Marty L., "Integrated modeling approach for an active optics system", Proc. SPIE 6271**,** 627116 (2006).

[6] Ansorge, W.,"VLT Environmental Specifications", VLT-SPE-ESO-10000-00004, rel. 5.0. (1993).

[7] EN 1998, Eurocode 8: Design of structures for earthquake resistance (1998).

[8] Perrotta, F., Schipani, P., "Filling the gap between FEM and control simulations in telescope project", Proc. SPIE 7017, 70171 (2008).